Hydrodynamic Interactions Between Two Slender Tori in a Viscous Fluid

Sangtae Kim
School of Chemical Engineering, Purdue University, 480 Stadium Mall Drive, West Lafayette, IN 47907

D. Palaniappan
Dept. of Mathematics & Statistics, Texas A&M University—Corpus Christi 6300 Ocean Drive, Corpus Christi, TX 78412

DOI 10.1002/aic.14403
Published online February 25, 2014 in Wiley Online Library (wileyonlinelibrary.com)

As a gift to Professor Bird, hydrodynamic interactions between two slender toroidal particles immersed in a viscous fluid are derived to extend the Rotne–Prager–Yamakawa (RPY) tensor formulation of bead-spring and bead-rod models of polymer kinetic theory to toroidal beads. As a relatively simple example of a multiply connected domain, this model geometry exhibits the special "role of the hole" and features new tensorial constructs beyond the Oseen–Burgers and Stokes quadrupoles that are encountered in the classical RPY theory. © 2014 American Institute of Chemical Engineers *AIChE J*, 60: 1517–1522, 2014

Keywords: complex fluids, fluid mechanics, microrheology, particulate flows, rheology

Introduction

Winters can be very cold in Madison, Wisconsin, with the temperatures reaching lows of -20°F in the early morning hours. Over a five-year period, that is, the relevant time scale for a typical Ph.D. student in chemical engineering, some of the luckier few may have even experienced -30°F en route to the very early (7:45 am) morning CHE725 lectures of Professor Bird. The senior author of this work (SK), as a young assistant professor 30 years ago, sat in those lectures and witnessed the large numbers (typically two or three dozen) of students who were attracted by the magical qualities of Professor Bird's lectures. Every seat in the classroom was occupied, except for those by the windows, as it was well known that Professor Bird liked to open the windows during the lecture! It may have been very cold outside, but in the classroom the "hot topics" in polymer kinetic theory as described in Dynamics of Polymeric Liquids[1] warmed the ears of many students. In this dedication, we honor those memories of the bead-spring and bead-rod models for polymer rheology.

The simplest versions of these models involved spherical beads that were simply points of frictional resistance to the fluid flow and thus, governed by the stokes law for the force on a sphere as covered in undergraduate courses in transport phenomena.[2] But in this advanced, 700-level course, hydrodynamic interactions (HI) were introduced promptly and thus, the bead–bead interactions changed from the simple Oseen–Burgers form

$$\boldsymbol{\Omega}^{(0)} = \frac{1}{8\pi\eta_s L}[\boldsymbol{\delta} + \boldsymbol{uu}] \tag{1}$$

to the more formidable Rotne–Prager–Yamakawa (RPY) form

$$\boldsymbol{\Omega} = \frac{1}{8\pi\eta_s L}\left\{\left(1+\frac{1}{6}\xi^2\right)\boldsymbol{\delta} + \left(1-\frac{1}{2}\xi^2\right)\boldsymbol{uu}\right\} \tag{2}$$

In these expressions, L denotes the distance between bead centers and $\boldsymbol{u}$ is a unit vector along the line of centers between the two beads. And in the expression for the RPY tensor, the parameter $\xi = d/L$ is the ratio between the bead diameters and the distance between the bead centers.

While the RPY tensor can be derived in a number of ways, one simple approach follows directly from the modeling of the bead–bead interactions using the properties for low-Reynolds-number (Stokes) flow past submerged spheres.[3] We first consider an isolated sphere of diameter d and center at $\boldsymbol{x}_1$ and note that its disturbance velocity field can be expressed in terms of the Oseen tensor, $\mathcal{G}$ (this term is also called the Stokeslet) and the Laplacian of the Oseen tensor, $\nabla^2\mathcal{G}$ (this term is also known as the degenerate Stokes quadrupole)

$$\boldsymbol{v}(\boldsymbol{x}) = \frac{1}{8\pi\eta_s}\boldsymbol{F}^{\text{ext}} \cdot \left\{1+\frac{d^2}{24}\nabla^2\right\}\mathcal{G}(\boldsymbol{x}-\boldsymbol{x}_1) \ , \quad \mathcal{G}(\boldsymbol{x}) = \frac{\boldsymbol{\delta}}{|\boldsymbol{x}|} + \frac{\boldsymbol{xx}}{|\boldsymbol{x}|^3} \tag{3}$$

The relationship between the external force (hydrodynamic drag) and bead motion is given by Stokes law so that $\boldsymbol{F}^{\text{hyd}} = -\boldsymbol{F}^{\text{ext}} = 3\pi\eta_s d(\boldsymbol{U}^{\infty} - \boldsymbol{U})$ where the last factor is the difference

Correspondence concerning this article should be addressed to S. Kim at kim55@purdue.edu.

between the ambient uniform stream and the sphere's translational velocity. This solution is equivalent to the solution that is more familiar to chemical engineers from Chapter 2 of Professors Bird, Stewart and Lightfoot's *Transport Phenomena*[2] as may be verified by conversions between Cartesian and spherical coordinates. The form given here is often called a singularity solution as it reveals that the disturbance produced by the sphere is precisely that of a point force or Green's function for Stokes flow, $(\mathcal{G}/8\pi\eta_s)$, the solution of the Stokes equation with the Dirac delta function forcing

$$-\nabla p+\eta_s\nabla^2\boldsymbol{v}=-\boldsymbol{F}^{\text{ext}}\,\delta(\boldsymbol{x})\ , \qquad \nabla\cdot\boldsymbol{v}=0 \tag{4}$$

plus a degenerate Stokes quadrupole

$$\nabla^2\mathcal{G}(\boldsymbol{x})=\frac{2\boldsymbol{\delta}}{|\boldsymbol{x}|^3}-\frac{6\boldsymbol{x}\boldsymbol{x}}{|\boldsymbol{x}|^5}\ . \tag{5}$$

On the sphere surface, $|\boldsymbol{x}|=d/2$, so that the $\boldsymbol{x}\boldsymbol{x}$ terms cancel in the singularity solution. The surviving terms, upon contraction between the force vector and the Kronecker delta unit tensor, $\boldsymbol{\delta}$, gives the required constant velocity on the sphere surface, $\boldsymbol{F}^{\text{ext}}/(3\pi\eta_s d)$ and Stokes Law when this constant vector is interpreted as $\boldsymbol{U}-\boldsymbol{U}^{\infty}$. This simple result for the sphere is analogous to the situation in potential theory (electrostatics) where the point charge solution is also the solution for a spherical conductor.

We then take the disturbance produced by bead 1 and consider its influence on bead 2. This is accomplished by use of the Faxen Law of low-Reynolds-number hydrodynamics which provides a direct relation between the mobility of a sphere centered at $\boldsymbol{x}_2$ (i.e., its translational velocity $\boldsymbol{U}$) immersed in an ambient velocity field $\boldsymbol{v}^{\infty}(\boldsymbol{x})$, the Stokes flow velocity that would exist in the absence of the sphere

$$\boldsymbol{F}^{\text{Hyd}}=3\pi\eta_s d\left\{1+\frac{d^2}{24}\nabla^2\right\}\boldsymbol{v}^{\infty}(\boldsymbol{x})\Big|_{\boldsymbol{x}=\boldsymbol{x}_2}-3\pi\eta_s d\ \boldsymbol{U} \tag{6}$$

If the ambient field is simply a uniform stream of constant velocity, $\boldsymbol{U}^{\infty}$, the Faxen Law simplifies to the more familiar Stokes Law, $3\pi\eta_s d(\boldsymbol{U}^{\infty}-\boldsymbol{U})$.

Combination of these two steps for beads 1 and 2 (while setting $\boldsymbol{F}^{\text{Hyd}}=0$ at bead 2) immediately leads to the RPY tensor (keeping in mind that $\nabla^2\nabla^2\mathcal{G}=0$, as velocity fields that satisfy the Stokes equations also satisfy the biharmonic equation, and $\boldsymbol{u}=(\boldsymbol{x}_2-\boldsymbol{x}_1)/|\boldsymbol{x}_2-\boldsymbol{x}_1|$)

$$\begin{aligned}\boldsymbol{U}_2&=\frac{\boldsymbol{F}^{\text{ext}}}{8\pi\eta_s}\cdot\left\{1+\frac{d^2}{24}\nabla^2\right\}\left\{1+\frac{d^2}{24}\nabla^2\right\}\mathcal{G}(\boldsymbol{x}-\boldsymbol{x}_1)\Big|_{\boldsymbol{x}=\boldsymbol{x}_2}\\&=\frac{\boldsymbol{F}^{\text{ext}}}{8\pi\eta_s}\cdot\left\{1+\frac{d^2}{12}\nabla^2\right\}\left\{\frac{\boldsymbol{\delta}}{|\boldsymbol{x}-\boldsymbol{x}_1|}+\frac{(\boldsymbol{x}-x_1)(\boldsymbol{x}-x_1)}{|\boldsymbol{x}-\boldsymbol{x}_1|^3}\right\}\Big|_{\boldsymbol{x}=\boldsymbol{x}_2}\\&=\frac{\boldsymbol{F}^{\text{ext}}}{8\pi\eta_s L}\cdot\left\{\left(1+\frac{1}{6}\xi^2\right)\boldsymbol{\delta}+\left(1-\frac{1}{2}\xi^2\right)\boldsymbol{u}\boldsymbol{u}\right\}\\&=\boldsymbol{F}^{\text{ext}}\cdot\boldsymbol{\Omega}(\boldsymbol{u};\xi).\end{aligned} \tag{7}$$

The key observation is that the special limit of the Oseen–Burgers tensor ($\xi=0$ in the RPY tensor) corresponds to approximating the disturbance field from bead 1 with just the Oseen tensor (neglecting the degenerate Stokes quadrupole) and using Stokes Law instead of the Faxen Law at bead 2.

The stage is, thus, set for beads of more exotic shapes. We look for singularity solutions that are analogs of those encountered for the sphere, namely a combination of Stokeslets and degenerate Stokes quadrupoles; and then apply the associated Faxen Laws for the mobility. The association between these two steps is in recognition of the shared functional form which is not a coincidence but rather a consequence of the Lorentz reciprocal theorem of low-Reynolds-number hydrodynamics.[3] For more general bead geometries, we will see that $\boldsymbol{\Omega}(\boldsymbol{u};\xi)$ should be generalized from a function of the two parameters (center–center orientation and ξ) to $\boldsymbol{\Omega}(\boldsymbol{x}_2,\boldsymbol{x}_1;d_2,d_1)$, centers and diameters of the reference beads.

The article is organized as follows. In the next section, we review the Stokes image system for the general ellipsoid and the associated Faxen relation for the mobility of the ellipsoid. This leads immediately to the extension of the RPY tensor to "ellipsoidal beads." While this result has been mentioned before, that is, in the same work that derived the ellipsoidal image system,[4] the repetition serves a useful purpose as it will set the context for new RPY-type expressions presented here for rings (slender "toroidal beads"). In Section 3, we derive the appropriate Stokes image system for a slender torus, taking special care to structure the result so as to preserve—to the extent possible—the historic, RPY-molded intuition preferred by the polymer physics community. Despite the obvious geometric differences between an ellipsoid and a torus, we find that the Stokes singularities can be distributed inside the torus so as to arrive at an image system that consists of Stokeslets and degenerate Stokes quadrupoles plus a small perturbation term associated with the multiply connected topology of the torus (associated with torques generated by flow through the hole in the torus). We are, thus, able to derive RPY interactions that are identical to the forms encountered for spherical and ellipsoidal beads plus a new term (new form) arising from the toroidal topology. We conclude this tribute article with some conjectures for the image system for low-Reynolds-number hydrodynamics of the general, that is, nonslender torus.

The Image System for the General Ellipsoid

Ellipsoidal beads are obvious model extensions for the case of anisotropic local environments. For the general ellipsoid with semiaxes a, b, and c (with $a\geq b\geq c$) oriented in the standard Cartesian coordinates (x,y,z), the disturbance velocity field in a uniform ambient stream can be written in terms of ellipsoidal harmonics and ellipsoidal coordinates as in the classical 1876 solution of Oberbeck.[5] This solution, the analog of the sphere solution in spherical coordinates, is prohibitively cumbersome as the pathway for the two-ellipsoid analysis. Alternatively, the solution may be written as an infinite series of Stokes singularities of higher order, that is, the spatial derivatives of the Stokeslet obtained by applying the differential operator

$$\frac{\sinh D}{D}=\sum_{k=0}^{\infty}\frac{D^{2k}}{(2k+1)!}=\sum_{k=0}^{\infty}\frac{(D^2)^k}{(2k+1)!} \tag{8}$$

and the nontermination of the series is a manifestation of the loss of spherical symmetry. Here, D^2 is the second-order differential operator in which the second derivatives of the Laplacian are weighted according to the ellipsoid geometry

$$D^2=a^2\frac{\partial^2}{\partial x^2}+b^2\frac{\partial^2}{\partial y^2}+c^2\frac{\partial^2}{\partial z^2} \tag{9}$$

For the special case of the sphere, $a=b=c$, the operator $D^2=a^2\nabla^2=(d^2/4)\nabla^2$ is proportional to the Laplacian and

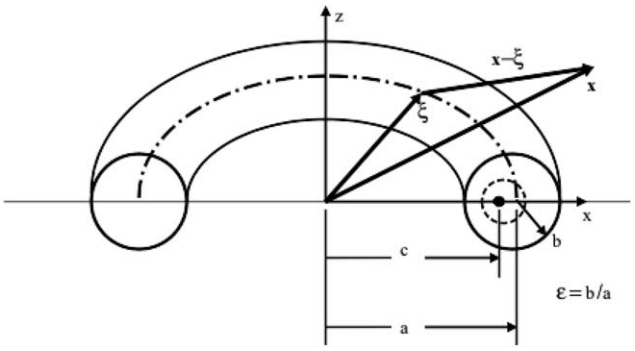

Figure 1. Toroidal geometry.

the infinite series truncates after only two terms (the Stokeslet and degenerate Stokes quadrupole) because $\nabla^2\nabla^2\mathcal{G}=0$ (the velocity fields that satisfy the Stokes equations also satisfy the biharmonic equation).

The general ellipsoid also possesses singularity solutions as derived in Kim and Arunachalam[4] with the same two terms as the sphere (Stokeslet and degenerate Stokes quadrupole) but now distributed along the focal ellipse (degenerate ellipse in the family of ellipsoids that are confocal to the ellipsoid of interest), that is

$$\begin{aligned}\boldsymbol{v}(\boldsymbol{x}) &= \frac{\boldsymbol{F}^{\text{ext}}\cdot}{8\pi\eta_s}\left(\frac{\sinh D}{D}\right)\mathcal{G}(\boldsymbol{x}) \\ &= \frac{\boldsymbol{F}^{\text{ext}}\cdot}{8\pi\eta_s}\int_{E(\boldsymbol{x}')} f(\boldsymbol{x}')\left\{1+\frac{c^2}{2}q^2\nabla^2\right\}\mathcal{G}(\boldsymbol{x}-\boldsymbol{x}')\ dA(\boldsymbol{x}')\end{aligned} \tag{10}$$

The proof of the equivalance of the infinite multipole series and the focal-distribution solution is provided as well in.[4] The Faxen law connecting the translational motion to the ambient field exhibits the same functional form over the focal ellipse

$$\boldsymbol{U}_2=\int_{E(\boldsymbol{x}')} f(\boldsymbol{x}')\left\{1+\frac{c^2}{2}q^2\nabla^2\right\}\boldsymbol{v}^{\infty}(\boldsymbol{x})|_{\boldsymbol{x}=\boldsymbol{x}'}\ dA(\boldsymbol{x}') \tag{11}$$

where

$$f(\boldsymbol{x})=\frac{1}{2\pi a_E b_E}q^{-1},\quad q(\boldsymbol{x})=\left(1-\frac{x^2}{a_E^2}-\frac{y^2}{b_E^2}\right)^{1/2}$$
$$a_E=(a^2-c^2)^{1/2},\quad b_E=(b^2-c^2)^{1/2}\ .$$

Thus, the final result for the RPY tensor for two ellipsoidal beads (after using again the biharmonic properties of the Oseen tensor) is

$$\begin{aligned}\boldsymbol{U}_2 &= \frac{1}{8\pi\eta_s}\boldsymbol{F}^{\text{ext}}\cdot\int_{E_2}\int_{E_1} f_2(\boldsymbol{x}_2')f_1(\boldsymbol{x}_1') \\ &\left\{1+\left(\frac{c_1^2q_1^2+c_2^2q_2^2}{2}\right)\nabla^2\right\}\mathcal{G}(\boldsymbol{x}-\boldsymbol{x}_1')|_{\boldsymbol{x}=\boldsymbol{x}_2'}\ dA(\boldsymbol{x}_1')dA(\boldsymbol{x}_2') \\ &= \boldsymbol{F}^{\text{ext}}\cdot\int_{E_2}\int_{E_1} f_2(\boldsymbol{x}_2')f_1(\boldsymbol{x}_1')\boldsymbol{\Omega}(\boldsymbol{x}_2',\boldsymbol{x}_1';2\sqrt{3}c_2q_2,2\sqrt{3}c_1q_1)\ dA_1dA_2\end{aligned} \tag{12}$$

We may summarize the steps leading to the RPY results for ellipsoidal beads as follows. The singularity solution for the ellipsoid consists of Stokeslets and degenerate Stokes quadrupoles distributed over the focal ellipse and confirms the intuition of "composite spherical bead assemblies" used in polymer kinetic theory. The associated Faxen law is a similar integral of the ambient velocity field, $\boldsymbol{v}^{\infty}$, and its Laplacian, $\nabla^2\boldsymbol{v}^{\infty}$, over the focal ellipse. The RPY tensor for HI between two ellipsoidal beads at arbitrary orientations takes the form of a double integral (analogous to view factors in radiative heat transfer) of the $\boldsymbol{\Omega}$ function between points on the respective focal ellipses and may be interpreted as a superposition of interactions between ellipsoids formed by composites of subspheres. The singularity solutions play a crucial role in the methodology because they furnish relatively simple forms expressed in laboratory coordinates. We will see in the next section that many of these ideas carry over to toroidal beads.

The Rotne-Prager-Yamakawa interactions for slender toroidal beads

Consider a torus formed by rotating about the z axis, a circle of radius b centered at $(a,0)$ in the xz-plane (see Figure 1). The most interesting limit is that of small $\epsilon=b/a$ because we want to consider the situations with appreciable flow through the "hole" of the torus. Analgous to the ellipsoid and as a shape that conforms to a standard coordinate system, the torus possesses classical Stokes flow solutions[6] in terms of eigenfunction expansions derived from toroidal harmonics. But here again, in comparison with the singularity solutions, these eigenfunctions are of limited utility in the analysis of two-body interactions.

Our search for a suitable set of Stokes singularities for slender "toroidal beads" is guided by our experience with the general ellipsoid. Our goal is to find an image system (areal distribution) that consists of a Stokeslet and a degenerate Stokes quadrupole, so that after combination with the Faxen relation we arrive at the familiar and recognizable form for the RPY tensor. However, we shall find that the topology of the torus, namely the hole and loss of the simply connected domain, introduces a novel twist so that the goal cannot be achieved. Nevertheless, we can achieve a partial victory by expressing the requisite vector fields as a primary component that involves just the desired singularities (Stokeslet, degenerate Stokes quadrupole) plus a small perturbation arising from the topological distinction.

The slender torus has two disparate length scales, namely a and b. The points in the fluid domain at great distances from the torus correspond to $|\boldsymbol{x}|\gg a$, and in this region the disturbance velocity field can be written as a multipole expansion about the center of the body. But closer to the torus, this is obviously not the appropriate solution form; indeed the geometric center of the body lies in the fluid domain! For those points that are far away from the toroidal surface in comparison to b, there are asymptotic solutions obtained from an application of slender body theory that are highly accurate in the limit of small ϵ.[7]

In the classical slender body theory of low-Reynolds-number hydrodynamics, a distribution of Stokeslets is placed along the centerline of the slender body; and thanks to the analysis by Johnson[7] we know that an even more accurate solution can be obtained by augmenting the Stokeslets with degenerate Stokes quadrupoles. For the slender torus, this line distribution is of course a "ring" distribution along the circular centerline C of the toroidal solid

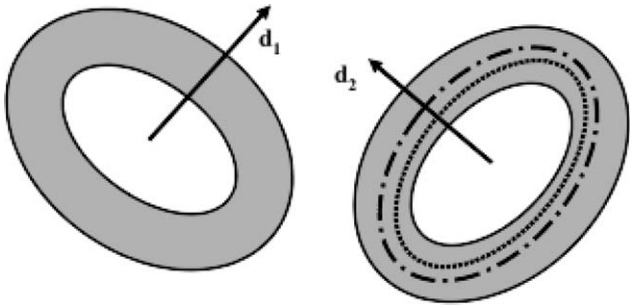

Figure 2. Two Tori (toruses) geometry.

$$\frac{\boldsymbol{F}^{\text{ext}}\cdot\boldsymbol{dd}\cdot}{8\pi\eta_s}\int_C\left[1+\frac{b^2}{4}\nabla^2\right]\mathcal{G}(\boldsymbol{x}-\boldsymbol{\xi})\frac{ds(\boldsymbol{\xi})}{2\pi a}$$
$$+\frac{\boldsymbol{F}^{\text{ext}}\cdot(\boldsymbol{\delta}-\boldsymbol{dd})\cdot}{8\pi\eta_s}\int_C\left\{\frac{2}{3}\hat{\boldsymbol{\xi}}\hat{\boldsymbol{\xi}}\hat{\boldsymbol{\xi}}+\frac{1}{3}(\boldsymbol{\delta}-\hat{\boldsymbol{\xi}}\hat{\boldsymbol{\xi}})\right\}\cdot\left[1+\frac{b^2}{4}\nabla^2\right]\mathcal{G}(\boldsymbol{x}-\boldsymbol{\xi})\frac{ds(\boldsymbol{\xi})}{\pi a}\tag{13}$$

In the solution presented above, we use the unit vector $\boldsymbol{d}$ to denote the axis of the torus; we use this instead of the z axis of Figure 1 so as to obtain forms that are more useful in the calculation of two-body interactions. The first line and second line correspond to axisymmetric (i.e., $\boldsymbol{F}^{\text{ext}}\parallel\boldsymbol{d}$) and edgewise (i.e., $\boldsymbol{F}^{\text{ext}}\perp\boldsymbol{d}$) flows, respectively, in the construct that students and colleagues of Professor Bird will recognize instantly from polymer kinetic theory. For the axisymmetric case, we have a uniform density of Stokeslets oriented in the flow direction as required by axisymmetry and integration of this force density over the circle (perimeter is $2\pi a$) produces the total force $\boldsymbol{F}^{\text{ext}}\cdot\boldsymbol{dd}$ as required. For the edgewise case (e.g., a uniform stream coming out of the page of Figure 1), the Stokeslet densities are determined by requiring a 2:1 ratio in the radial and tangential strengths as dictated by slender body theory and the normalization condition of recovering the total force $\boldsymbol{F}^{\text{ext}}\cdot(\boldsymbol{\delta}-\boldsymbol{dd})$ upon integration of the density distribution over the circular centerline.

The associated Faxen law for the force on a slender torus in an arbitrary ambient field is

$$\boldsymbol{F}^{\text{hyd}}=\eta_s A^{\parallel}\boldsymbol{dd}\cdot\int_C\left[1+\frac{b^2}{4}\nabla_{\xi}^2\right]\boldsymbol{v}^{\infty}(\boldsymbol{\xi})\frac{ds(\boldsymbol{\xi})}{2\pi a}-\eta_s A^{\parallel}\boldsymbol{dd}\cdot\boldsymbol{U}$$
$$+\eta_s A^{\perp}(\boldsymbol{\delta}-\boldsymbol{dd})\cdot\int_C\left\{\frac{2}{3}\hat{\boldsymbol{\xi}}\hat{\boldsymbol{\xi}}\hat{\boldsymbol{\xi}}+\frac{1}{3}(\boldsymbol{\delta}-\hat{\boldsymbol{\xi}}\hat{\boldsymbol{\xi}})\right\}\cdot\left[1+\frac{b^2}{4}\nabla_{\xi}^2\right]\boldsymbol{v}^{\infty}(\boldsymbol{\xi})\frac{ds(\boldsymbol{\xi})}{\pi a}$$
$$-\eta_s A^{\perp}(\boldsymbol{\delta}-\boldsymbol{dd})\cdot\boldsymbol{U}\tag{14}$$

where $A^{\parallel}$ and $A^{\perp}$ are the resistance functions for axisymmetric and edgewise motions. Set $\boldsymbol{F}^{\text{hyd}}=0$ and solve for $\boldsymbol{U}$

$$\boldsymbol{U}=\boldsymbol{dd}\cdot\int_C\left[1+\frac{b^2}{4}\nabla_{\xi}^2\right]\boldsymbol{v}^{\infty}(\boldsymbol{\xi})\frac{ds(\boldsymbol{\xi})}{2\pi a}$$
$$+(\boldsymbol{\delta}-\boldsymbol{dd})\cdot\int_C\left\{\frac{2}{3}\hat{\boldsymbol{\xi}}\hat{\boldsymbol{\xi}}\hat{\boldsymbol{\xi}}+\frac{1}{3}(\boldsymbol{\delta}-\hat{\boldsymbol{\xi}}\hat{\boldsymbol{\xi}})\right\}\cdot\left[1+\frac{b^2}{4}\nabla_{\xi}^2\right]\boldsymbol{v}^{\infty}(\boldsymbol{\xi})\frac{ds(\boldsymbol{\xi})}{\pi a}\tag{15}$$

The RPY tensor is obtained using the disturbance from bead 1 as the ambient field near bead 2 (Figure 2), that is, insertion of the velocity field from Eq. 13 into Eq. 15, and will lead to double line integrals that are reminiscent of the double area integrals for the ellipsoid, Eq. 12

$$\int_{C2}\int_{C1}(\qquad)\left[1+\frac{b_1^2+b_2^2}{4}\nabla^2\right]\mathcal{G}(\boldsymbol{x}-\boldsymbol{x}_1')|_{x=x_2'}ds_1ds_2\tag{16}$$

with a very long but straightforward expression in the parentheses involving the dot products of terms in $\boldsymbol{d}_2\boldsymbol{d}_2$ and $(\boldsymbol{\delta}-\boldsymbol{d}_2\boldsymbol{d}_2)$ for bead 2 with terms in $\boldsymbol{d}_1\boldsymbol{d}_1$ and $(\boldsymbol{\delta}-\boldsymbol{d}_1\boldsymbol{d}_1)$ for bead 1.

Further refinements of the slender body approximation are possible as shown in Johnson and Wu[8] and lead to singularity solutions that are accurate to $O(\epsilon^2\log\epsilon)$. In analogy with the placement of higher order multipoles at the center of a simply connected particle, we may add Stokes dipoles and higher multipoles in the circular ring. The need for the Stokes dipole can be explained with simple physics by considering the HI between "distal" portions of the torus and a reference point where the no-slip boundary condition is applied.

We use Figure 1 and consider the HI between the local region and the distal portion of the torus. Or equivalently and perhaps easier on our intuition, we consider the implications of the relatively stagnant region in the hole vs. the faster flow in the outer (exposed) portion of the torus. The imputed velocity gradient between the "inner" and "outer" regions has the classical decomposition into the rate-of-strain field and the vorticity field in yet another reminder of the cold Wisconsin mornings with Professor Bird (CHE-620 or CHE-720)! These two fields are responsible for inducing stresslets (symmetric Stokes dipole) and rotlets (antisymmetric Stokes dipole) velocity fields

$$\frac{1}{2}(\boldsymbol{F}^{\text{ext}}\hat{\boldsymbol{\xi}}+\hat{\boldsymbol{\xi}}\boldsymbol{F}^{\text{ext}})\cdot\nabla\mathcal{G}(\boldsymbol{x}-\boldsymbol{\xi})=\frac{1}{|\boldsymbol{x}-\boldsymbol{\xi}|^3}\boldsymbol{F}^{\text{ext}}$$
$$\cdot\boldsymbol{\xi}(\boldsymbol{x}-\boldsymbol{\xi})-\frac{3}{|\boldsymbol{x}-\boldsymbol{\xi}|^5}\boldsymbol{F}^{\text{ext}}\cdot(\boldsymbol{x}-\boldsymbol{\xi})\;\;\boldsymbol{\xi}\cdot(\boldsymbol{x}-\boldsymbol{\xi})(\boldsymbol{x}-\boldsymbol{\xi})$$
$$\frac{1}{2}(\boldsymbol{F}^{\text{ext}}\hat{\boldsymbol{\xi}}-\hat{\boldsymbol{\xi}}\boldsymbol{F}^{\text{ext}})\cdot\nabla\mathcal{G}(\boldsymbol{x}-\boldsymbol{\xi})$$
$$=\frac{1}{|\boldsymbol{x}-\boldsymbol{\xi}|^3}\left[\boldsymbol{F}^{\text{ext}}\cdot(\boldsymbol{x}-\boldsymbol{\xi})\hat{\boldsymbol{\xi}}-\hat{\boldsymbol{\xi}}\cdot(\boldsymbol{x}-\boldsymbol{\xi})\boldsymbol{F}^{\text{ext}}\right],$$

respectively, along the centerline of the torus as deduced by Johnson[7] (for a general background singularity solutions in low-Reynolds-number flow we refer the reader to Kim and Karrila[3]).

We now arrive at the crucial point of departure from the prior work of Johnson[7,8] in our efforts to preserve the standard RPY forms. We will extend the image system beyond the centerline ring and this will remove most of the Stokes dipole. Let the position vector $\boldsymbol{c}$ denote a point on the focal ring along the same radial line as the point $\boldsymbol{\xi}$ on the centerline. We note that $\boldsymbol{\xi}-\boldsymbol{c}=(a-c)\;\hat{\boldsymbol{\xi}}=(1/2)\epsilon b\;\hat{\boldsymbol{\xi}}$ (see Appendix). But a displacement of the Stokeslet location by a small amount can be expressed in a Taylor series whose first two terms are a Stokeslet at the original location plus a Stokes dipole

$$\mathcal{G}_{ij}(\boldsymbol{x}-\boldsymbol{\xi})=\mathcal{G}_{ij}(\boldsymbol{x}-\boldsymbol{c})-(\boldsymbol{\xi}-\boldsymbol{c})\cdot\nabla\mathcal{G}_{ij}(\boldsymbol{x}-\boldsymbol{c})+\ldots$$
$$=\mathcal{G}_{ij}(\boldsymbol{x}-\boldsymbol{c})-(\xi-c)_k\mathcal{G}_{ij,k}(\boldsymbol{x}-\boldsymbol{c})+\ldots$$
$$=\mathcal{G}_{ij}(\boldsymbol{x}-\boldsymbol{c})-\frac{1}{2}\epsilon b\;\hat{\xi}_k\left[\frac{1}{2}\left(\mathcal{G}_{ij,k}+\mathcal{G}_{ik,j}\right)+\frac{1}{2}\left(\mathcal{G}_{ij,k}-\mathcal{G}_{ik,j}\right)\right]+\ldots$$

where we have used $\nabla_{\xi}\mathcal{G}_{ij}(\boldsymbol{x}-\boldsymbol{c})=-\nabla\mathcal{G}_{ij}(\boldsymbol{x}-\boldsymbol{c})$ in the first line. At this point, it is convenient to handle the

axisymmetric and edgewise cases separately, to facilitate the comparisons with the results in[7].

Axisymmetric Flows. In axisymmetric flows, $\boldsymbol{F}^{\text{ext}} \parallel \boldsymbol{d}$ and by symmetry the Stokeslets with this axial orientation are distributed with uniform strengths along the ring. We write $\boldsymbol{F}^{\text{ext}} = F^{\parallel}\boldsymbol{d}$ in this section to simplify the notation and consider the implications for the leading terms in the Taylor series written as a difference between two Stokeslets, namely, a Stokeslet on the centerline ring and a Stokeslet on the focal ring

$$F^{\parallel} d_j \mathcal{G}_{ij}(\boldsymbol{x}-\boldsymbol{\xi}) - F^{\parallel} d_j \mathcal{G}_{ij}(\boldsymbol{x}-\boldsymbol{c}) = \left(-\frac{\epsilon b}{2}\right) F^{\parallel} d_j \hat{\xi}_k \left[\frac{1}{2}\left(\mathcal{G}_{ij,k}+\mathcal{G}_{ik,j}\right)+\frac{1}{2}\left(\mathcal{G}_{ij,k}-\mathcal{G}_{ik,j}\right)\right] \tag{17}$$

For the stresslet, this is indeed the finding in Johnson[7] (see page 24, where the strength of the stresslet is found to be $-(\epsilon b/2)$ times the strength of the Stokeslet; Johnson's expression does not have the minus sign because his definition of the stresslet uses an opposite sign convention).

For the rotlet, Johnson has

$$\left(-\frac{\epsilon b}{2}+\frac{\epsilon \log(8/\epsilon)\ b}{2}\right) F^{\parallel} d_j \hat{\xi}_k \frac{1}{2}\left(\mathcal{G}_{ij,k}-\mathcal{G}_{ik,j}\right) \tag{18}$$

and, thus, the $O(\epsilon)$ term is again identified with the difference between two Stokeslets located on the centerline and focal rings. Conversely, $O(\epsilon \log \epsilon)$ term is an "intrinsic rotlet" associated with the hole/topology of the torus—any shift in a Stokeslet would lead to equal stresslet-rotlet combinations and the stresslet does not have an $O(\epsilon \log \epsilon)$ term.

We may summarize the axisymmetric case as follows. In place of Eq. 13, we have the improved result to higher order accuracy

$$\frac{F^{\parallel}\boldsymbol{d}\cdot}{8\pi\eta_s}\left\{\int_C 2\left[1+\frac{b^2}{4}\nabla^2\right]\mathcal{G}(\boldsymbol{x}-\boldsymbol{\xi})\frac{ds(\boldsymbol{\xi})}{2\pi a}-\int_F\left[1+\frac{b^2}{4}\nabla^2\right]\mathcal{G}(\boldsymbol{x}-\boldsymbol{c})\frac{ds(\boldsymbol{c})}{2\pi c}\right\} + \frac{\epsilon\log(8/\epsilon)\ b}{2}\frac{F^{\parallel}}{8\pi\eta_s}\int_C d_j\hat{\xi}_k\ \frac{1}{2}\left(\mathcal{G}_{ij,k}(\boldsymbol{x}-\boldsymbol{\xi})-\mathcal{G}_{ik,j}(\boldsymbol{x}-\boldsymbol{\xi})\right)\frac{ds(\boldsymbol{\xi})}{2\pi a} \tag{19}$$

where the labels C and F in the integrals denote the centerline and focal rings (see Appendix A), respectively.

The Faxen law (for the component in the axisymmetric $\boldsymbol{d}$-direction) follows in an analogous fashion to Eq. 15 except that the integrals are now over both rings (with the appropriate weighting factors (2 for C-ring and -1 for the F-ring) and there is a new term that contains the vorticity of the ambient field

$$\boldsymbol{dd}\cdot\frac{\epsilon\log(8/\epsilon)\ b}{2}\int_C(\nabla\times\boldsymbol{v}^{\infty}(\boldsymbol{\xi}))\times\hat{\boldsymbol{\xi}}\ \frac{ds(\boldsymbol{\xi})}{2\pi a} \tag{20}$$

Edgewise Flows. For edgewise flows the same ideas are encountered, namely the stresslet distribution on the C-ring can be removed by placing opposing Stokeslets on the F- and C-rings, and the rotlet has a $\epsilon\log\epsilon$ term that is not present in the stresslet.

But there is one new wrinkle, namely the 2:1 ratio seen in the leading-order slender body theory, Eq. 13 is lost at the higher order and the factor

$$\frac{2}{3}\hat{\boldsymbol{\xi}}\hat{\boldsymbol{\xi}}+\frac{1}{3}(\boldsymbol{\delta}-\hat{\boldsymbol{\xi}}\hat{\boldsymbol{\xi}}) \tag{21}$$

becomes

$$\left[\frac{2}{3}-\frac{2}{3(6L-17)}\right]\hat{\boldsymbol{\xi}}\hat{\boldsymbol{\xi}}+\left[\frac{1}{3}+\frac{2}{3(6L-17)}\right](\boldsymbol{\delta}-\hat{\boldsymbol{\xi}}\hat{\boldsymbol{\xi}}),\quad L=\log(8/\epsilon) \tag{22}$$

Thanks to the curvature in the torus, the Stokeslet in the radial direction is slightly less and that in the tangential direction is slightly more than that predicted at the leading order.

General Flows. We combine the axisymmetric and edgewise cases to get the general solution. The main results pertain to the singularity solution and the Faxen laws and these are summarized below

$$\begin{aligned}\boldsymbol{v}(\boldsymbol{x}) = {}& \frac{\boldsymbol{F}^{\text{ext}}\cdot\boldsymbol{dd}\cdot}{8\pi\eta_s}\int_{2C-F}\left[1+\frac{b^2}{4}\nabla^2\right]\mathcal{G}(\boldsymbol{x}-\boldsymbol{\xi})\frac{ds(\boldsymbol{\xi})}{P}\\ &+\frac{\boldsymbol{F}^{\text{ext}}\cdot\boldsymbol{d}}{8\pi\eta_s}\frac{\epsilon\log(8/\epsilon)\ b}{2}\int_C d_j\hat{\xi}_k\ \frac{1}{2}(\mathcal{G}_{ij,k}(\boldsymbol{x}-\boldsymbol{\xi})-\mathcal{G}_{ik,j}(\boldsymbol{x}-\boldsymbol{\xi}))\frac{ds(\boldsymbol{\xi})}{P}\\ &+\frac{\boldsymbol{F}^{\text{ext}}\cdot(\boldsymbol{\delta}-\boldsymbol{dd})\cdot}{8\pi\eta_s}\int_{2C-F}\left\{\left[\frac{2}{3}-\frac{2}{3(6L-17)}\right]\hat{\boldsymbol{\xi}}\hat{\boldsymbol{\xi}}+\left[\frac{1}{3}+\frac{2}{3(6L-17)}\right](\boldsymbol{\delta}-\hat{\boldsymbol{\xi}}\hat{\boldsymbol{\xi}})\right\}\\ &\cdot\left[1+\frac{b^2}{4}\nabla^2\right]\mathcal{G}(\boldsymbol{x}-\boldsymbol{\xi})\frac{ds(\boldsymbol{\xi})}{P/2}\\ &+\frac{1}{8\pi\eta_s}\frac{\epsilon\log(8/\epsilon)\ b}{2}\int_C F_j^{\perp}\hat{\xi}_k\ \frac{1}{2}(\mathcal{G}_{ij,k}(\boldsymbol{x}-\boldsymbol{\xi})-\mathcal{G}_{ik,j}(\boldsymbol{x}-\boldsymbol{\xi}))\frac{ds(\boldsymbol{\xi})}{P}\end{aligned} \tag{23}$$

where we have used the notation $2C-F$ to denote the weighted integrations over the double-ring, P to denote the perimeter of each ring and $F_j^{\perp}$ to denote the j-th component of the force vector $\boldsymbol{F}^{\text{ext}}\cdot(\boldsymbol{\delta}-\boldsymbol{dd})$ for the edgewise case.

The Faxen law for the velocity on a force-free torus (Appendix B) is

$$\begin{aligned}\boldsymbol{U} = {}& \boldsymbol{dd}\cdot\int_{2C-F}\left[1+\frac{b^2}{4}\nabla_{\xi}^2\right]\boldsymbol{v}^{\infty}(\boldsymbol{\xi})\frac{ds(\boldsymbol{\xi})}{P}\\ &+(\boldsymbol{\delta}-\boldsymbol{dd})\cdot\int_{2C-F}\left\{\left[\frac{2}{3}-\frac{2}{3(6L-17)}\right]\hat{\boldsymbol{\xi}}\hat{\boldsymbol{\xi}}+\left[\frac{1}{3}+\frac{2}{3(6L-17)}\right](\boldsymbol{\delta}-\hat{\boldsymbol{\xi}}\hat{\boldsymbol{\xi}})\right\}\\ &\cdot\left[1+\frac{b^2}{4}\nabla_{\xi}^2\right]\boldsymbol{v}^{\infty}(\boldsymbol{\xi})\frac{ds(\boldsymbol{\xi})}{P/2}\\ &+\frac{\epsilon\log(8/\epsilon)\ b}{2}\int_C(\nabla\times\boldsymbol{v}^{\infty}(\boldsymbol{\xi}))\times\hat{\boldsymbol{\xi}}\ \frac{ds(\boldsymbol{\xi})}{P}\end{aligned} \tag{24}$$

The extension of the RPY formula to slender toroidal beads follows from Eq. 24 for the Faxen law at bead 2 using the disturbance field from bead 1, Eq. 23, as the ambient field. The RPY is formed by the usual Stokeslet and degenerate Stokes quadrupole interactions plus a new term corresponding to ring-ring integrals of the vorticity of the Oseen–Burgers tensor.

Conclusions

The nature of bead-bead HI has been investigated for beads that are more exotic than the standard spheres encountered in Professor Bird's well known text on polymer kinetic theory and fluid dynamics. More specifically, the RPY tensor formulation has been extended to beads that are in the shape of slender tori, with the primary objective of elucidating the effect of multiply-connected domains (the "role of the hole") on HI. This was achieved by methods for calculating particle–particle HI in low-Reynolds-number flow, specifically our construction of the Stokes singularity representation of

the disturbance from one bead and the extraction of its influence on the mobility of the second bead via the Faxen law.

We have demonstrated one key aspect in the development of the RPY formulas from low-Reynolds-number fluid dynamics, namely, the importance of the choice of the image system. The standard RPY tensor (for spherical beads) arises from the Stokeslet and degenerate Stokes quadrupole combination in the image system consisting of the point at the sphere center. For the slender torus (and in general, other particles of nonspherical shape), the singularity solution at some standard reference point would take the form of a multipole expansion, that is, an infinite series instead of a two-term expansion. But when the singularities are distributed on the double-ring consisting of two concentric circles, the centerline and the focal ring, the result is a singularity solution that consists of the desired Stokeslet and degenerate Stokes quadrupole combination plus a small correction consisting of a rotlet distributed on the centerline ring. The end result is that the nontrivial geometric and topological aspects of the slender torus can be visualized as a superposition of primary microbeads strung together on the centerline, secondary microbeads on the focal ring (that impart momentum opposite to the beads on the primary ring) and tertiary microbeads spinning about axes tangential to the centerline.

As closing remarks, we share with the readers that the SK worked on these ideas during the closing months of his first era at the University of Wisconsin (1983–1997) as part of a greater effort on the search for singularity solutions for the general (i.e., nonslender) torus with image systems bounded between the centerline and focal rings. Over the subsequent years, as a participant in the pharmaceutical research community, computer-aided drug design took priority over work on microhydrodynamics. Ongoing societal trends that emphasize translational research over curiosity-driven research will continue to constrain the pace of discovery in microhydrodynamics, including our efforts to find singularity solutions and the image system for the general (e.g., nonslender) toroid. This special effort in honor of Professor Bird's 90th birthday is an occasion to celebrate the creation of new insights in the spirit of search for knowledge that may help others develop new directions in rheological models.

Appendix A: Toroidal Coordinates

We define and use the toroidal coordinate system in this appendix to derive several geometric relationships that are relevant for the image system. We follow a common convention and assign the z axis as the axis of symmetry and define toroidal coordinates (σ, τ, ϕ) as

$$x = c\frac{\sinh\tau}{\cosh\tau - \cos\sigma}\cos\phi \tag{A1}$$

$$y = c\frac{\sinh\tau}{\cosh\tau - \cos\sigma}\sin\phi \tag{A2}$$

$$z = c\frac{\sin\sigma}{\cosh\tau - \cos\sigma} \tag{A3}$$

so that surfaces of constant τ are tori with their centerlines (rings) on the xy-plane. The cross-section of the torus in a meridional half-plane (e.g., the xz-plane with $x \geq 0$) is a circle centered at $(a,0)=(c\coth\tau, 0)$ of radius $b=c/\sinh\tau$. The role of the parameter c can be seen by taking the limit of large τ; the torus degenerates into the "focal ring" or "focal circle" of radius c in the xy-plane whose cross-section in the meridional half-plane is the point $(c,0)$.

For the slender torus, we following the notation in Johnson[7] and introduce the small parameter $\epsilon = b/a$, that is, the ratio of cross-sectional radius b and the "hoop" radius a. As this is associated with large values of τ, we note that

$$\epsilon = \frac{b}{a} = \frac{c}{\sinh\tau}\frac{\sinh\tau}{c\cosh\tau} = \frac{1}{\cosh\tau} = 2e^{-\tau} + O(\epsilon^3) \tag{A4}$$

This small parameter ϵ also appears as the ratio of the distance between the rings a–c and the cross-sectional radius b, that is

$$\frac{a-c}{b} = (c\coth\tau - c)\frac{\sinh\tau}{c} = \cosh\tau - \sinh\tau = e^{-\tau} = \frac{1}{2}\epsilon + O(\epsilon^3) \tag{A5}$$

Appendix B: Faxen Law for a Force-Free Particle

Chapter 3 of Kim and Karrila[3] provides a derivation of the Faxen Law as a consequence of the Lorentz reciprocal theorem. Specifically for the purposes of this present work, if a particle of arbitrary shape possesses a singularity solution of the form

$$v_i(\boldsymbol{x}) = \eta_s A_{jk} U_k \mathcal{F}\{\mathcal{G}_{ij}/(8\pi\eta_s)\} \tag{B1}$$

where $\mathcal{F}$ is a linear functional (e.g., integral and/or differential operator) and $\eta_s A_{jk}$ are the components of the resistance tensor, then the hydrodynamic force for that particle moving with a translational velocity $\boldsymbol{U}$ in an arbitrary ambient velocity field $\boldsymbol{v}^\infty(\boldsymbol{x})$ is given by the Faxen Law expression

$$-\boldsymbol{F}^{\text{ext}} = \boldsymbol{F}^{\text{Hyd}} = \eta_s \boldsymbol{A}\cdot\mathcal{F}\{\boldsymbol{v}^\infty\} - \eta_s \boldsymbol{A}\cdot\boldsymbol{U} \tag{B2}$$

For the force-free (neutrally buoyant) case, we set $\boldsymbol{F}^{\text{Hyd}} = 0$ to get

$$\boldsymbol{U} = \boldsymbol{A}^{-1}\cdot\boldsymbol{A}\cdot\mathcal{F}\{\boldsymbol{v}^\infty\} = \mathcal{F}\{\boldsymbol{v}^\infty\} \tag{B3}$$

which is a very simple result. Thus for the neutrally buoyant ellipsoid and torus, the Faxen law for the translational velocity is a simple integral of the ambient velocity field over the image system without explicit appearance of elliptic integrals and toroidal harmonics that otherwise occur in the resistance tensor.

Literature Cited

1. Bird RB, Armstrong RC, Hassager O. Dynamics of Polymeric Liquids, Vol. 1, *Fluid Dynamics*, 2nd ed. New York: Wiley, 1987.
2. Bird RB, Stewart WE, Lightfoot EN. *Transport Phenomena*, 2nd ed. New York: Wiley, 2002.
3. Kim S, Karrila SJ. *Microhydrodynamics: Principles and Selected Applications*, Boston: Butterworth-Heinemann, 1991.
4. Kim S, Arunachalam K. The general solution for an ellipsoid in low-Reynolds number flow. *J Fluid Mech.* 1987;178:535–547.
5. Oberbeck A. *Crelles J.* 1876;81:62.
6. Payne LE, Pell WH. The Stokes flow problem for a class of axially symmetric bodies. *J Fluid Mech.* 1960;7:529–549.
7. Johnson RE. Slender-body theory for Stokes flow and flagellar hydrodynamics. Ph. D. Thesis, California Institute of Technology, Pasadena, CA, 1977.
8. Johnson RE, Wu TY. Hydromechanics of low-Reynolds-number flow. *Part 5. Motion of a slender torus. J Fluid Mech.* 1979;95:263–277.

Manuscript received Oct. 10, 2013, and final revision received Feb. 3, 2014.